Electronic Supplementary Information

Electrochemical Synthesis of H_2O_2 on BiNiOx-4 and In-situ Disinfection

Yizhen Shao[a], Yanfei Fei[b], Ge Feng [a], Shijie Zhang[a] , Xiaoge Peng[a] , Chenghang Jiang[a], Yuanan Li[a], ZhongTing Hu[b] , Zhikang Bao[a,*] and Jianguo Wang[a,*]

[a]Institute of Industrial Catalysis, State Key Laboratory Breeding Base of Green-Chemical Synthesis Technology, College of Chemical Engineering, Zhejiang University of Technology, Hangzhou 310032, P.R. China.

[b]College of Environment, Zhejiang University of Technology, Hangzhou, 310032, P. R. China

[*]Correspondence and requests for materials should be addressed to Z.K.B (email: zkbao@zjut.edu.cn), or to J.G.W. (email: jgw@zjut.edu.cn).

1. Materials and methods

1.1. materials

Bismuth trinitrate ($Bi(NO_3)_3 \cdot 5H_2O$, Macklin, AR 99.9%), Nickel acetate ($Ni(OAc)_2 \cdot 4H_2O$, Macklin, AR 99.9%), Urea ($CO(NH_2)_2$, Aladdin, AR 98%), Citric acid ($C_6H_8O_7$, Aladdin, AR 97%), Nafion solution (DuPont), Dipotassium titanium oxide dioxalate ($K_2TiO(C_2O_4)_2$, Aladdin, AR 98%), Sulfuric acid (H_2SO_4, Lingfeng Chemical Reagent Co., Ltd, AR 99.9%), Potassium hydroxide (KOH, Sinopharm Chemical Reagent Co., Ltd, AR 99.5%), Ethanol (CH_3CH_2OH, Sinopharm Chemical Reagent Co., Ltd, AR 99.5%), Deionized water (DI, Millipore 18.2 MΩ cm^{-1}), hydrogen peroxide (H_2O_2, Alfa Aesar, 35% w/w).

1.2. Bacterial strains

Model bacteria selected are Gram-negative *Pseudomonas aeruginosa* (*P. aeruginosa*) Boston 41501 (ATCC27853) and *Escherichia coli* (*E. coli*) FDA strain Seattle 1946 (ATCC25922), and Gram-positive *Staphylococcus aureus* (*S. aureus*) FAD209 (ATCC6538) in this study. All bacterial strains were routinely sustained in TSB medium with 25% glycerol at -80 ℃.

1.3. Material characterizations

The scanning electron microscope (SEM) equipment is Phenom ProX with field emission. The transmission electron microscope (TEM, Tecnai G2F30S-Twin) is operated at 300 kV. The test procedure is: Disperse the sample on a carbon-coated copper net, dry it under infrared light, and observe it directly. Use STEM (FEI Titan G2 80-200 ChemiSTEM) to observe the energy dispersive X-ray spectrum (EDX). X- ray powder diffraction (XRD) was performed on an X-ray

diffractometer (PANalytical X-pert Pro) with Cu Ka irradiation (λ = 1.5418 Å) at 40 kV and 40 mA. The sample's X-ray photoelectron spectroscopy (XPS) is tested by X-ray photoelectron spectroscopy (Thermo Scientific K-Alpha) with a monochromated Al Kα (1486.6 eV) radiation source. For the XPS measurements, the powder samples were pelletized to remove the effect of the carbon tape substrate in the XPS spectra. XPS deconvolution was conducted using XPSPeak41 software. Shirley-type background removal and mixed Gaussian– Lorentzian (70:30) functions were used for deconvolution. The metal content in the catalysts was quantified by Inductively Coupled Plasma Optical Emission Spectrometer (ICP-OES, PerkinElmer). The O contents in the samples were determined using combustion elemental analysis (EA, Flash 2000, Thermo Fisher Scientific) based on the dynamic flash combustion method.

1.4. Electrochemical details

All electrochemical performance tests are carried out on the electrochemical workstation (CHI 760, Shanghai Chenhua Instrument Co., Ltd.), including the selective performance test and yield test of the electrocatalytic oxygen reduction reaction to generate hydrogen peroxide. The same uses the traditional three-electrode system: the working electrode (WE) is a drop-cast electrode, the counter electrode (CE) is a platinum wire or stable anode (MMO), and the saturated calomel electrode (SCE) is used as the reference electrode (RE). To evaluate the selectivity of the catalyst and the number of electrons transferred, a rotating ring disk electrode (RRDE-3A, ALS Co., Ltd) device was used, including a glassy carbon (GC) disk (diameter 4 mm) surrounded by a Pt ring (inner diameter 5 mm, outer diameter 7 mm) electrode. Before use, the electrode was polished on elk leather (PK-3, ALS Co., Ltd) with a uniformly dispersed 0.05μm alumina

suspension (Gaoss Union, Inc.), then washed with pure water ultrasonically and under ambient conditions.

For RRDE (selectivity and transfer number): To prepare working electrodes of drop-casted BiNiOx-4, the same amount (~4 mg) of BiNiOx-4 powders was suspended in the 1:9 (v/v) mixture (Total volume was 1mL) of Nafion solution (DuPont D520, 5 wt%) and absolute ethanol by sonicating for 60 min. The obtained solution was called catalysts "ink". Then, 5.0 μL of homogeneous "ink" was slowly dispersed on the GC area of RRDE electrode and then dried under infrared light.

To better compare potentials, all the reported potentials were referred to as the reversible hydrogen electrode (RHE) potential, according to pH values of O_2-saturated electrolytes.

$$E(RHE) = E(SCE) + 0.0591 \times pH + 0.241V$$

Unless otherwise specified, the E mentioned in this article were relative to the RHE.

First, the electrochemical oxygen reduction reaction occursin a single electrolytic cell with 60 mL of electrolyte (0.1 M KOH). Before the measurement, let in O_2 gas at a flow rate of 30 sccm for at least 30 min, to make the electrolyte saturated with oxygen. During the measurement process, O_2 remains unchanged, and the oxygen concentration in the electrolyte is always at the maximum. The H_2O_2 selectivity (%) and the electron transfer number (n) was calculated based on the current of both disk and ring electrodes (Equation (1)). And the corresponding electron transfer number (n) can also be obtained by Equation 2.

$$H_2O_2\% = 200 \times \frac{I_R/N}{I_D + I_R/N} \quad (1)$$

$$n = 4 \times \frac{I_R/N}{I_D + I_R/N} \quad (2)$$

For Flow-cell (yield): To evaluate the output (yield) of hydrogen peroxide, the method adopted by the working electrode: spray the catalyst dispersion containing a certain amount of nafion solution directly on the diffusion layer (Suzhou Shengernuo, YLS-30T), and use the whole as a working electrode, The purpose is to obtain more siginificant current. The effective area of this experimental device (Flow cell, **Fig.S10**) is 3 × 3cm. Use scissors to cut the diffusion layer into small pieces of 3 cm × 3 cm as the working area, and spray the catalyst dispersion on the diffusion layer to obtain the corresponding cathode electrode. The anode electrode directly uses commercially available stable metal oxide anode materials (MMO, $IrO_2Ta_2O_5$-Ti).

The H_2O_2 production performance was evaluated using a homemade electrolytic cell (Flow-cell), which employed a constant current method with a fixed current for 120 min at a time. The anode and cathode chambers were separated by NEPEM-115 membrane (Jiangsu Kairun Membrane Material Co., Ltd.) or FAB-PK-130 (fumasep) cut into small pieces (4 cm × 4 cm). The laboratory electrolyte was circulated with 0.1 M KOH (0.5 M Na_2SO_4, 0.5 M H_2SO_4) at a flow rate of 30 mL min^{-1}, and the working electrode consisted of catalysts and diffusion layers sprayed with different loadings (0.05 mg cm^{-2}~0.2 mg cm^{-2}). In addition, O_2 was fed into the flow cell at a rate of 30 mL min^{-1}. After the electrolysis process, the concentration of the generated H_2O_2 was tested by the potassium titanate oxalate color method.

We use the classical potassium titanate oxalate color method. This method is based on the formation of titanium (IV)-peroxide complexes in the presence of sulfuric acid. The detailed procedure of this method can be described as follows: a certain volume (1 ml) of the sample to be

tested is added to a solution of potassium titanate oxalate $K_2TiO(C_2O_4)_2$ (0.5 M, 1 ml) and 0.5 M H_2SO_4 solution (1 ml) prepared as before, and then the color of the solution changes to yellow due to the above-mentioned coloring reaction. Next, the UVvis technique (at 400 nm) was used to determine and calculate the amount of H_2O_2 in the samples.

The following equations can describe the relationships of Faradaic efficiency in Flow cell setup:

$$Faradaic\ efficiency\ (\%) = 100\ \times \frac{2\ \times C\ \times V\ \times F}{Q}$$

Here, C is the produced H_2O_2 concentration (mol L^{-1}), V is the volume of electrolyte (L), F is the faraday constant (96485 C/mol), Q is the passed charge amount (C).

1.5. Computational Methods.

All computations were carried out within the framework of the generalized gradient approximation (GGA) with the Perdew-Burke-Ernzerhof (PBE)[1] functional in the Vienna ab initio simulation program (VASP)[2, 3]. The cutoff energy for the plane wave basis sets was 400 eV. A Gaussian smearing method with a width of 0.05 eV was applied. The convergence criteria of geometry were set to be 0.02 eV/Å and the electronic energy of the supercell was set to be 10^{-6} eV. The Bi_2O_3 (a = 11.33 Å, b = 11.33 Å, c = 5.55 Å) with 24 O atoms and 16 Bi atoms was built and optimized. The gamma-centered k-point mesh was adopted for all Bi_2O_3 surfaces. In order to avoid interactions between adjacent slabs, the vacuum layer of 15 Å was placed along the z-direction. The pristine Bi_2O_3 (010) surface, the pristine NiO (100) surface, and Bi_2O_3 (010) with Ni-doped (denoted as Ni_x-Bi_2O_3, x represents the number of Ni atoms) surface were adopted to this study.

The O_2 adsorption energy was investigated for the Ni_x-Bi_2O_3 surface:

$$\Delta E_{O2-ads} = E_{O2*} - E_{O2} - E_{pristine}$$

where E_{O2*} is the energy of the optimized structure with O_2 adsorption, and $E_{pristine}$ is the energy of the pristine Bi_2O_3 slab. For 2e- ORR, the reaction path is as follows[4]:

$$O_2 + * + H^+ + e^- \rightarrow OOH^*$$

$$OOH^* + H^+ + e^- \rightarrow HOOH^*$$

And the free energy of each step was calculated with the following equation:

$$\Delta G = \Delta E + \Delta ZPE - T\Delta S - neU$$

where ΔE is the energy calculated by DFT, and U is the applied potential for the reaction. The thermodynamic correction was considered by calculating zero-point energy (ZPE) and entropy (S). For adsorbates, all 3N degrees of freedom of intermediate species were treated as harmonic vibrations, and the entropies were calculated as a sum of the contributions from these vibrational motions. For gaseous molecules, the entropy was calculated from NIST-JANAF thermochemical tables. The limiting potential of $2e^-$ ORR is the highest potential that makes each reaction step exothermic, which can be defined by the following equation:

$$U_L{}^{2e-\ ORR} = \min [\Delta G_1{}^0, \Delta G_2{}^0]/e$$

$$\eta = 0.70 - U_L{}^{2e-\ ORR}$$

where $\Delta G_1{}^0$ and $\Delta G_2{}^0$ are the free energies of each $2e^-$ ORR at U =0.00 V, and η is the theoretical over-potential.

1.6. Bactericidal tests

The study employed Pseudomonas aeruginosa as the model pathogens for the bactericidal activity test. Frozen stock of P. aeruginosa was inoculated onto a TSA plate and incubated at 37 °C for 24 h in a ZHICHENG ZXDP-B2050 incubator oven. A single colony of P. aeruginosa was subsequently inoculated into 20 mL TSB broth and cultivated in a shaking incubator (120 rpm, Honour HNY-200B) at 37 °C for 18 h. The bacterial cells were then harvested through centrifugation and washed with a phosphate-buffered saline (PBS, 0.01M, pH 7.2) solution before being resuspended in PBS at a cell density of 10^8 colony forming units per mL (CFU mL^{-1}).

The bactericidal effect of H_2O_2 produced at different concentrations and times was examined. To investigate the bactericidal effect of H_2O_2 at different concentrations, 20 mL PBS suspension

containing P. aeruginosa (~10^6 CFU mL^{-1}) was stirred in the presence of the calculated H_2O_2 and maintained at room temperature. At designated time intervals, 1 mL of the P. aeruginosa solution was withdrawn, diluted in PBS solution, and spread on an agar plate. The plate was then incubated at 37 °C for 24 h. In testing the bactericidal effect of H_2O_2 produced at different times, 200 μL of P. aeruginosa (~10^8 CFU mL^{-1}) suspension was added to 20 mL of H_2O_2 produced at different times, stirred and kept at room temperature. At designated time intervals, 1 mL of the P. aeruginosa solution was withdrawn, diluted in PBS solution, and spread on an agar plate. The plate was incubated at 37 °C for 24 h. Similar bactericidal tests were conducted on Escherichia coli and Staphylococcus aureus.

All experiments were conducted in a clean workbench (AIRTECH SW-CJ-1FD), and all consumables used were sterilized at 121 °C for 15 min in a STIK CO. LTD IMJ-85A autoclave or under UV radiation (254 nm) for 20 min. At least three replicates of the experiments were carried out to ensure accuracy and consistency of the results.

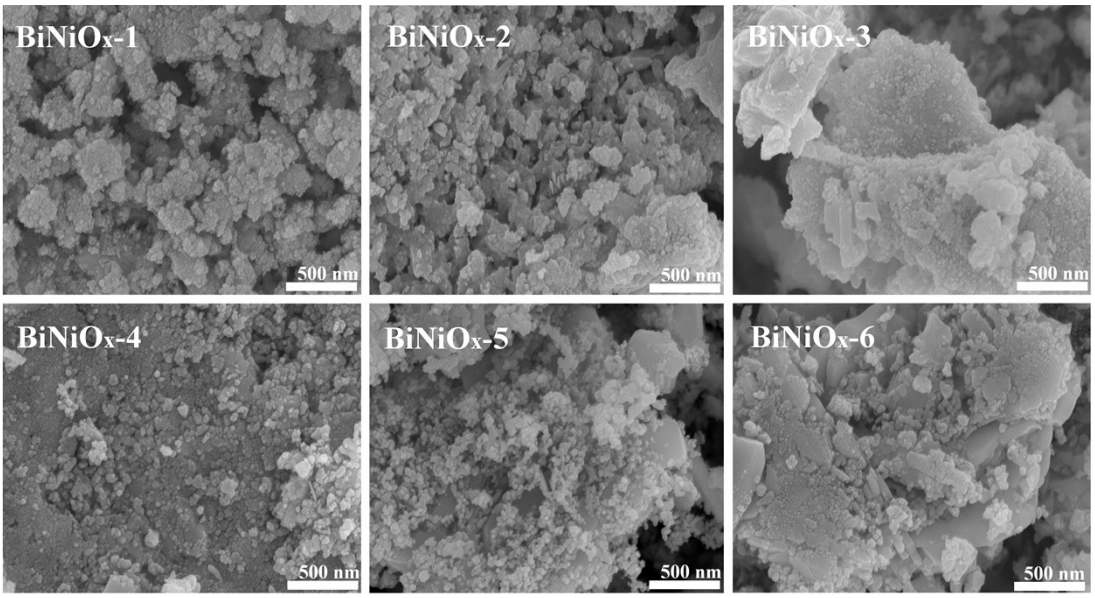

Fig. S1. The SEM images of BiNiOx-n.

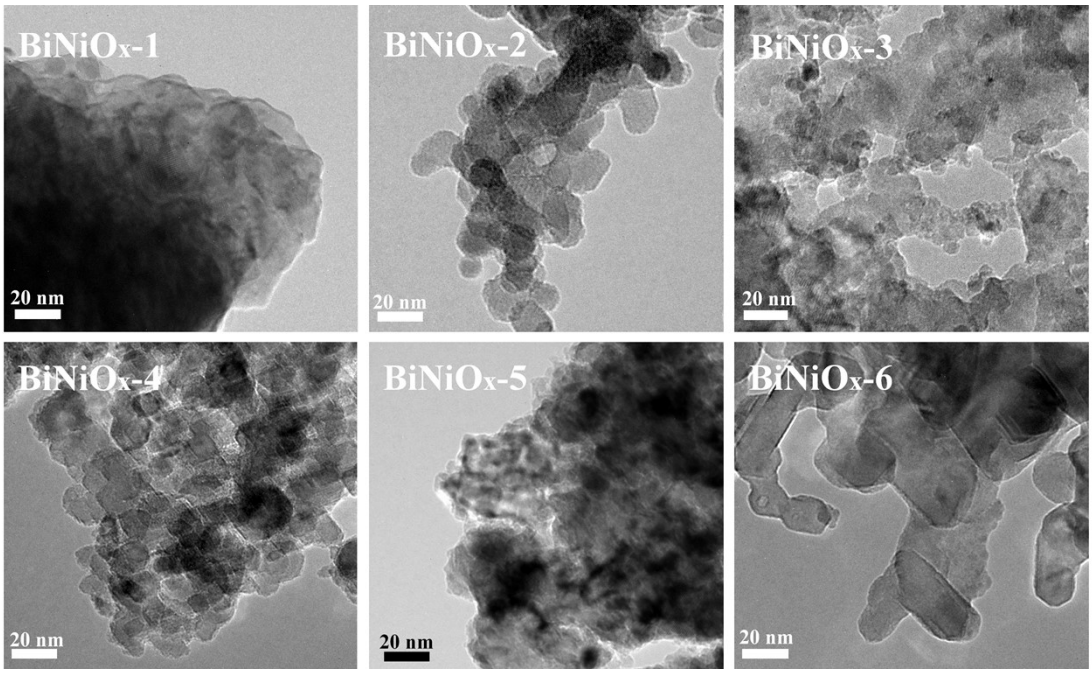

Fig. S2. The TEM images of BiNiOx-n.

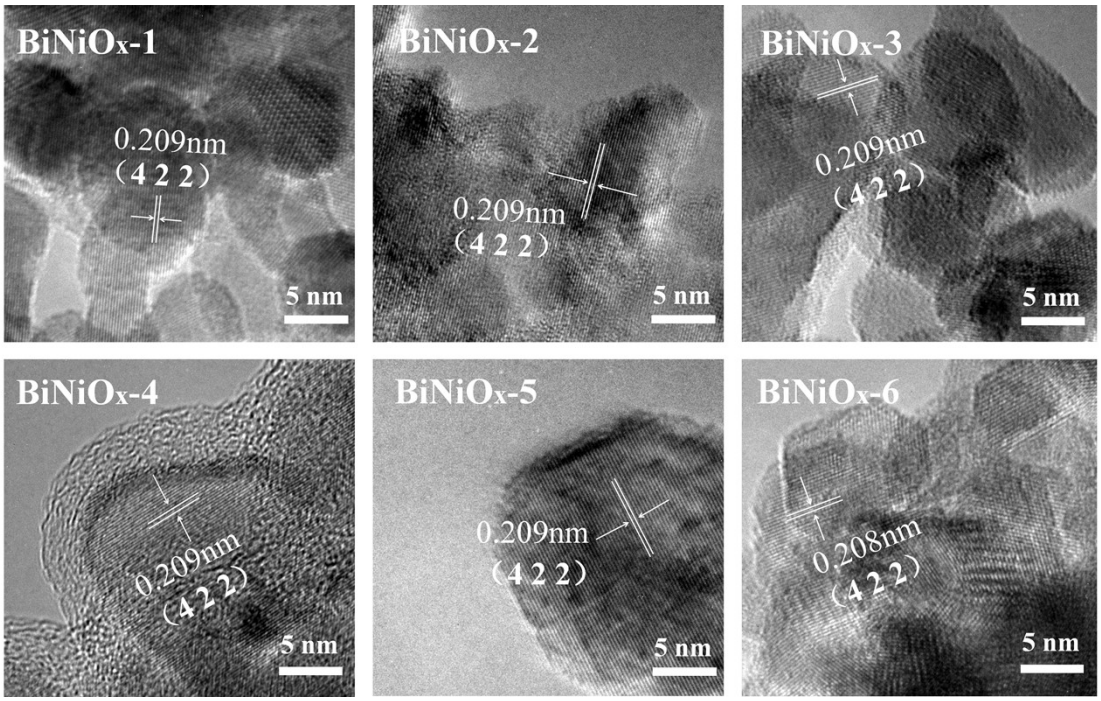

Fig. S3. The HR-TEM images of BiNiOx-n, corresponding to (422) crystal plane.

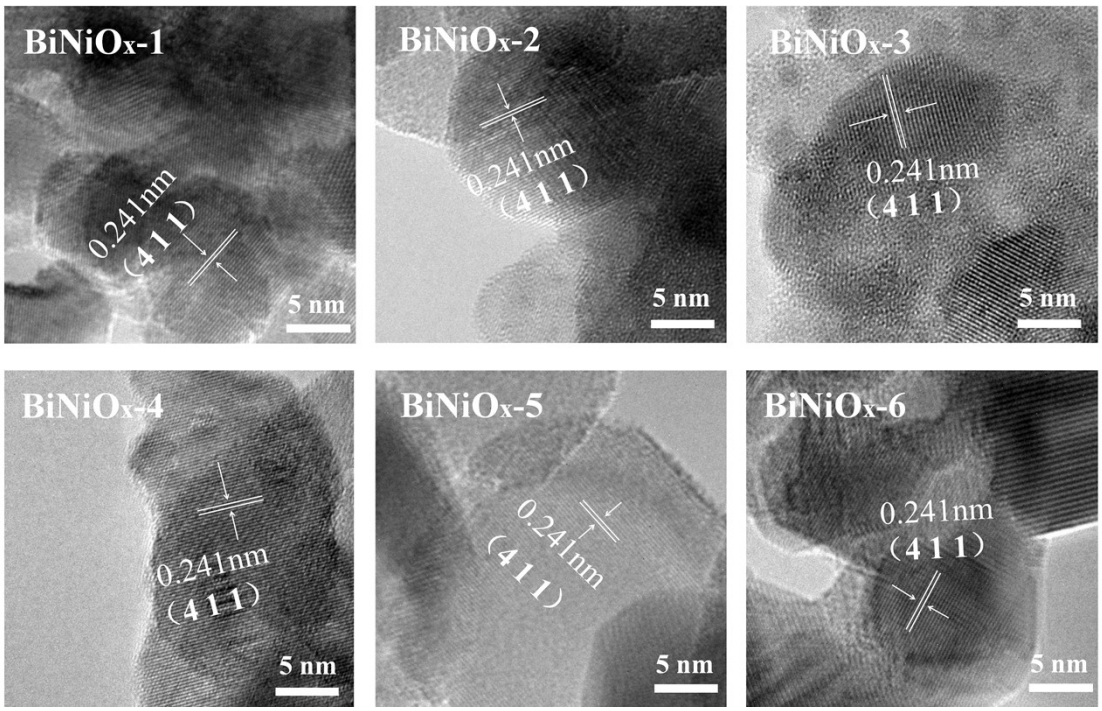

Fig. S4. The HR-TEM images of BiNiOx-n, corresponding to (411) crystal plane.

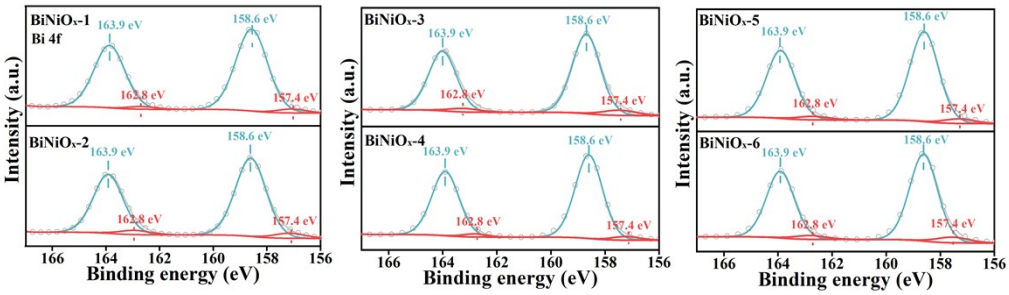

Fig. S5. The XPS of Bi 4f peaks of BiNiOx-n.

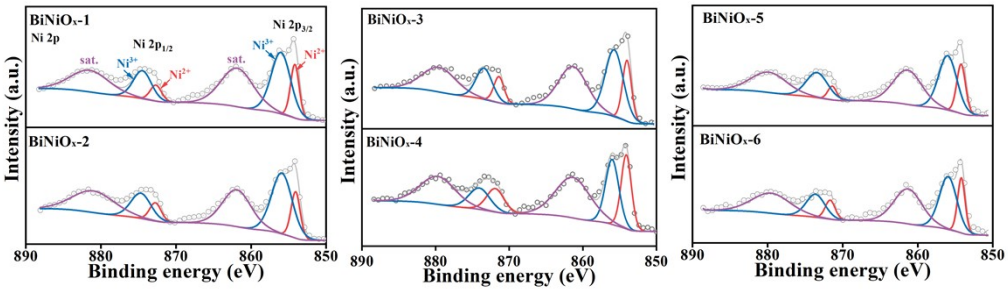

Fig. S6. The XPS of Ni 2p peaks of BiNiOx-n.

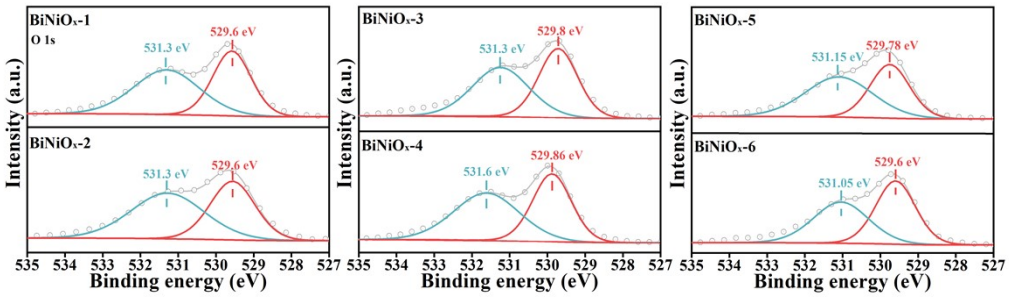

Fig. S7. The XPS of O 1s peaks of BiNiOx-n.

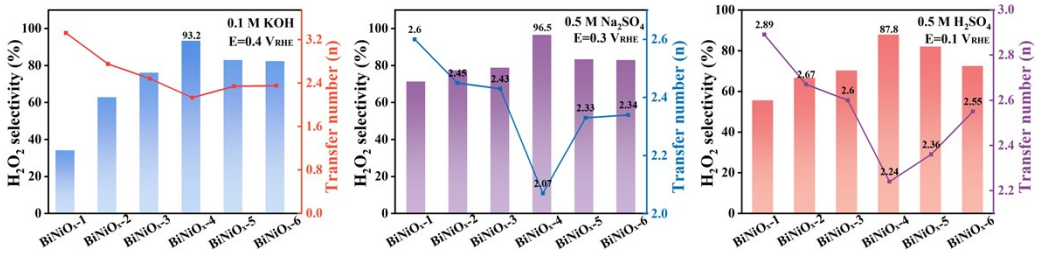

Fig. S8. H_2O_2 selectivity and electron number of BiNiOx-n at different pH.

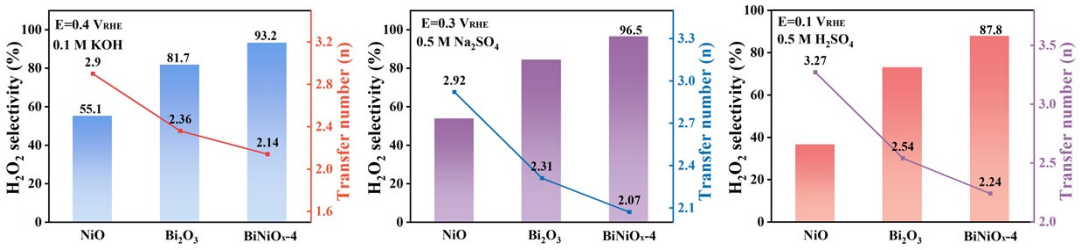

Fig. S9. H_2O_2 selectivity and electron number of Bi_2O_3 and NiO at different pH.

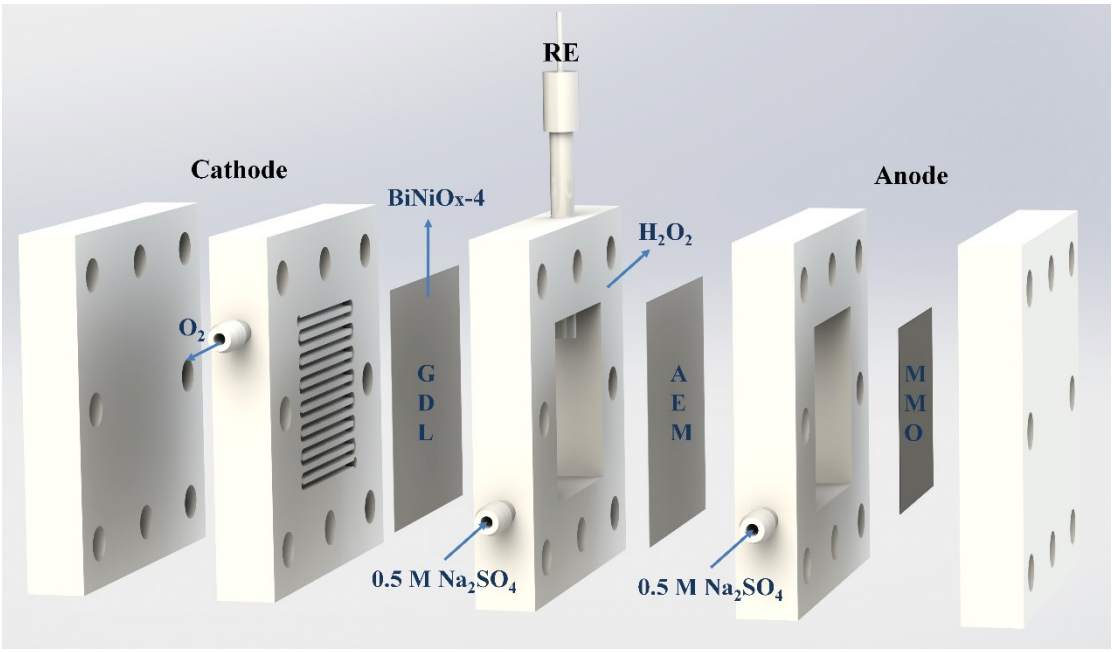

Fig. S10. Yield testing unit：Flow-cell.

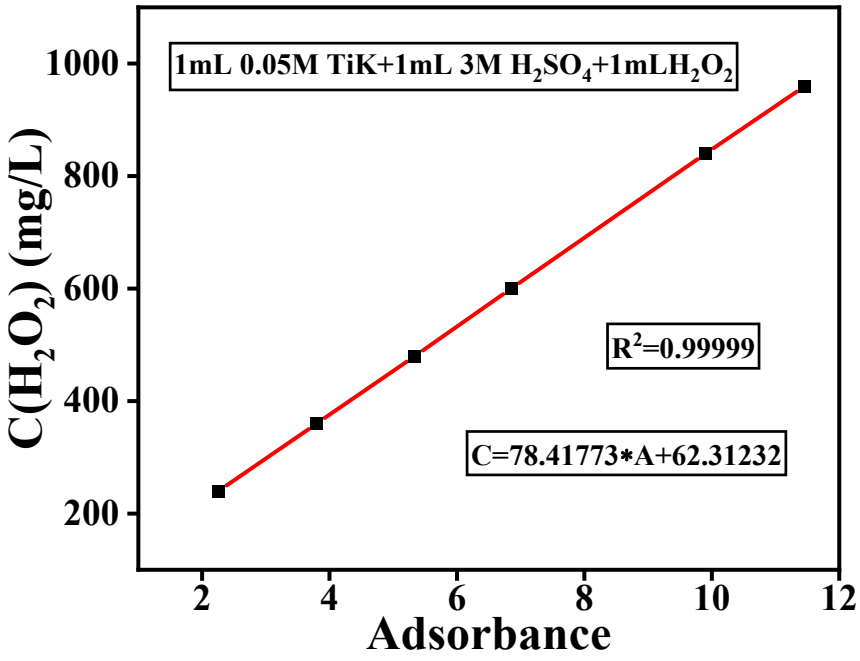

Fig. S11. The calibration curve of $K_2TiO(C_2O_4)_2$ solution and the standard curve of its reaction with hydrogen peroxide.

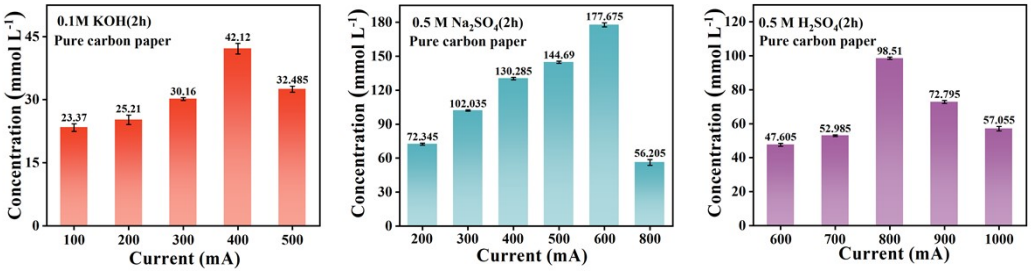

Fig. S12. The H_2O_2 production of pure carbon paper at different pH conditions and current.

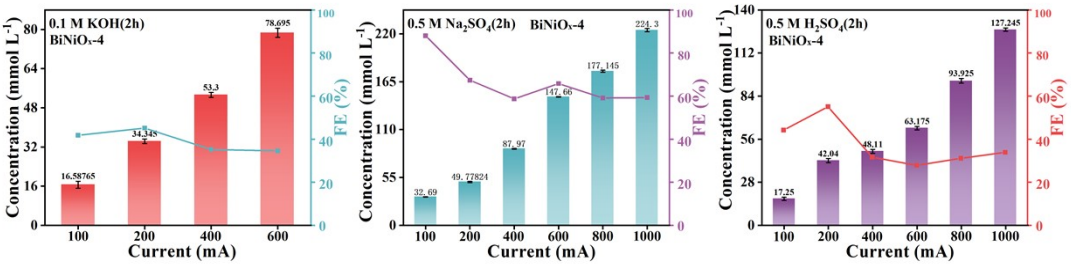

Fig. S13. The H_2O_2 production and FE of BiNiOx-4 at different pH conditions and current.

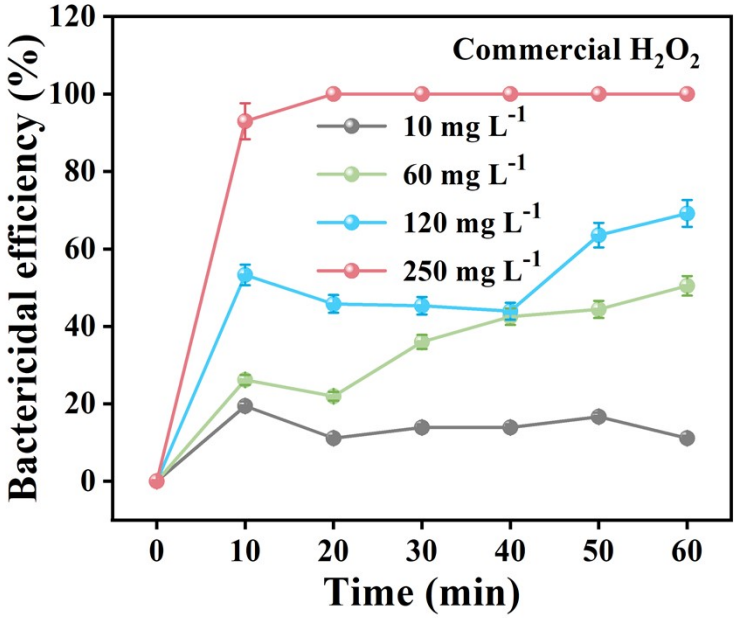

Fig. S14. Bactericidal effect of commercial hydrogen peroxide

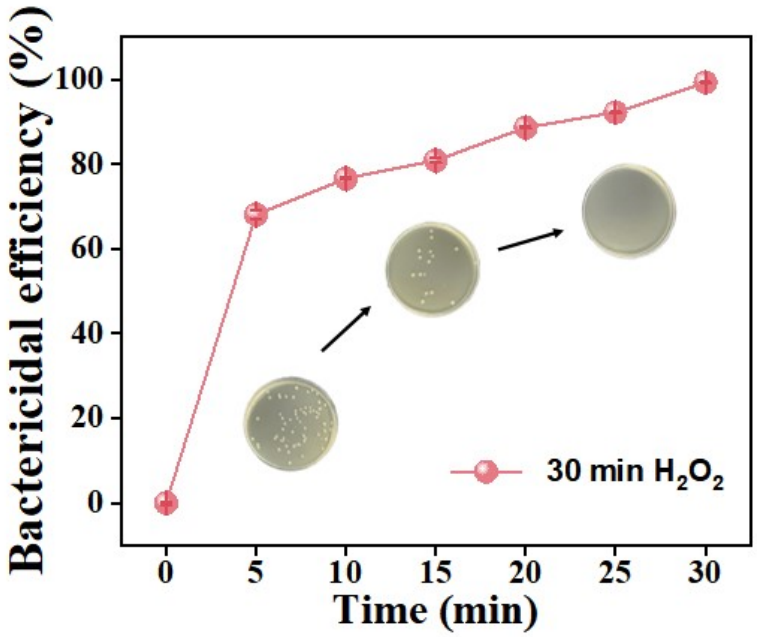

Fig. S15. The killing effect curve of H_2O_2 with 30 min on P. aeruginosa.

Table S1. The metal content of $BiNiO_x$-n (n=1, 2, 3, 4, 5, 6) obtained from ICP-OES and O content obtained from EA analysis

Samples	Bi loading (mol. %)	Ni loading (mol. %)	O loading (mol. %)	Bi:Ni
$BiNiO_x$-1	6.63	30.21	45.42	0.22:1
$BiNiO_x$-2	13.41	27.60	39.40	0.49:1
$BiNiO_x$-3	26.83	35.47	44.40	0.76:1
$BiNiO_x$-4	21.49	20.87	52.00	1.03:1
$BiNiO_x$-5	19.46	12.47	51.57	1.56:1
$BiNiO_x$-6	19.61	9.00	49.11	2.18:1

Table S2. Elemental compositions of $BiNiO_x$-4 obtained from EDX analysis

Samples	Bi loading (mol. %)	Ni loading (mol. %)	O loading (mol. %)
$BiNiO_x$-4	31.39	31.79	36.82

Table S3. Elemental compositions of $BiNiO_x$-n obtained from XPS analysis

Samples	Bi (Atomic %)	Ni (Atomic %)	O (Atomic %)	C (Atomic %)
$BiNiO_x$-1	4.13	23.92	46.89	25.06
$BiNiO_x$-2	8.11	16.33	48.18	27.38
$BiNiO_x$-3	9.49	10.97	43.71	35.83
$BiNiO_x$-4	12.22	10.17	46.69	30.92
$BiNiO_x$-5	13.55	10.30	44.08	32.07
$BiNiO_x$-6	14.32	8.95	38.62	38.11

Table S4. Concentrations of nickel species from XPS in BiNiOx-4 and NiO.

Samples	**Ni^{2+} (at%)**	**Ni^{3+} (at%)**	**ratio**
$BiNiO_x$-4	32.43	67.57	0.48：1
NiO	38.27	61.73	0.62：1

Table S5. Comparison of catalysts under different conditions

Reference	Catalysts	pH/electrolyte	Potential (V_{RHE})	H_2O_2 selectivity [%]
2	NPC	0.1 M KOH	-0.25-0.25	85
25	CMK-3	0.1 M KOH	0.4-0.6	90
26	Pt/C	0.1 M KOH	0.10	5
46	NiNx/C-$AQNH_2$	0.1 M KOH	0.2-0.8	80
47	GOMC	0.1 M KOH	0.2-0.8	90
47	H-GOMC	0.1 M KOH	0.2-0.8	92
48	CNTs	0.1 M KOH	0.6	60
48	O-CNTs	0.1 M KOH	0.6	90
49	Pure C	0.1 M KOH	0.4	82
49	P–C	0.1 M KOH	0.4	88
49	B–C	0.1 M KOH	0.4	84
51	g-N-CNHs	pH=13	0.5	20
13	Co-NC	0.1 M $HClO_4$	0.6	91
20	Pt-ZTC	0.1 M $HClO_4$	0.1-0.7	28
46	CMK-3	0.1 M HClO4	0.3	83

1. Perdew, J. P.; Burke, K.; Ernzerhof, M., *Physical Review Letters* 1996**, 77** (18), 3865-3868.
2. Kresse, G.; Furthmüller, J., *Computational Materials Science* 1996**, 6** (1), 15-50.
3. Kresse, G.; Furthmüller, J., *Physical Review B* 1996**, 54** (16), 11169-11186.
4. Chen, S.; Luo, T.; Chen, K.; Lin, Y.; Fu, J.; Liu, K.; Cai, C.; Wang, Q.; Li, H.; Li, X.; Hu, J.; Li, H.; Zhu, M.; Liu, M., *Angewandte Chemie International Edition* 2021**, 60** (30), 16607-16614.